




# Low-Energy Supernovae Bounds on Sterile Neutrinos

Garv Chauhan <sup>1</sup>, Shunsaku Horiuchi <sup>1,2</sup>, Patrick Huber<sup>1</sup> and Ian M. Shoemaker <sup>1</sup>

<sup>1</sup>*Center for Neutrino Physics, Department of Physics, Virginia Tech, Blacksburg, VA 24061, USA*

<sup>2</sup>*Kavli Institute for the Physics and Mathematics of the Universe (WPI), University of Tokyo, Chiba 277-8583, Japan*

Sterile neutrinos can be produced through mixing with active neutrinos in the hot and dense core of a core-collapse supernova (SN). The standard bounds on the active-sterile mixing ( $\sin^2 \theta$ ) from SN arise from SN1987A energy-loss, requiring  $E_{\text{loss}} < 10^{52}$  erg. In this letter, we discuss a novel bound on sterile neutrino parameter space arising from the energy deposition through its decays inside the SN envelope. Using the observed underluminous SN IIP population, this energy deposition is constrained to be below  $\sim 10^{50}$  erg. Focusing on sterile neutrino mixing only with the tau neutrino, for heavy sterile masses  $m_s$  in the range 100-500 MeV, we find stringent constraints on  $\sin^2 \theta_\tau$  reaching two orders of magnitude lower than those from the SN1987A energy-loss argument. Similar bounds will also be applicable to sterile mixing only with muons ( $\sin^2 \theta_\mu$ ).

**Introduction.** Although a great deal has been determined about neutrinos, the origin of neutrino mass remains unknown. A particularly simple possibility is that the Standard Model (SM) is augmented with at least two right-handed neutrinos which are singlets under SM interactions. As a result, such states can generate Dirac masses through nonzero Yukawa couplings to the SM lepton doublet and the Higgs, as well as Majorana masses at an unknown scale. After electroweak symmetry breaking, the left- and right-handed neutrinos mass mix, which effectively endows the “sterile neutrinos” with a suppressed coupling to the weak force, where the suppression is controlled by the mixing angles. In addition to accounting for neutrino masses, sterile neutrinos may play a role in unravelling other mysteries as well, including acting as a dark matter candidate [1, 2], and providing an origin for the observed baryon asymmetry [3].

In the face of significant theoretical uncertainty regarding the masses of sterile neutrinos, a wide range of varying experimental and theoretical probes have been brought to bear on the existence of sterile neutrinos over many orders of magnitude in mass (e.g., [4–7]). Such searches include colliders, beta decays, accelerators, as well as astrophysical and cosmological signatures.

In the present paper, we investigate the impact of 10-500 MeV scale sterile neutrinos on supernovae (SNe). Our work differs from previous studies on sterile neutrinos produced in SNe in several ways. In Refs. [8, 9] it was found that  $\sim 100$  MeV scale sterile neutrinos can transport large quantities of energy and augment the explosion. Moreover strong limits on sterile neutrinos have been derived on the argument that excessive energy loss would catastrophically shorten the neutrino burst, in contradiction with observations; this has been applied to eV [10, 11], keV [12–16], and  $\sim 100$  MeV scale sterile neutrinos [8, 9, 17–19].

Here however we derive strong constraints on sterile neutrinos based on the argument that they do not deposit more energy in the stellar envelope than what is observed in underluminous Type IIP SNe. Thus the lowest energy SNe yet observed will provide the strongest constraints. Similar arguments have been studied in axions [20].

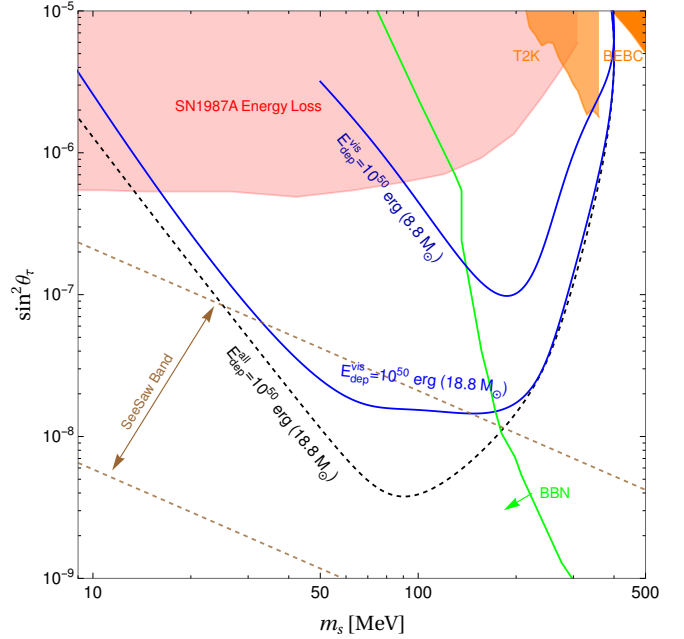


Figure 1. Bounds on sterile-active mixing  $\sin^2 \theta_\tau$  as a function of sterile mass  $m_s$ . The dashed black curve shows the low-energy SN bound assuming full energy deposition from decaying sterile inside the SN envelope ( $18.8M_\odot$ ), while the solid blue curves denotes the bound arising from energy deposition through visible decay channels only (shown for an Fe core  $18.8M_\odot$  progenitor and a ONeMg core  $8.8M_\odot$  progenitor, as labeled). The red-shaded region is the bound from energy loss in SN1987A [19]. Other displayed constraints include BBN bounds assuming standard cosmology [21–23], T2K [24], and BEBC bounds [25].

As such, we extend the SM to include a heavy sterile neutrino  $\nu_s$  which interacts with the SM exclusively via the type I seesaw Lagrangian [26–28],

$$\mathcal{L} \supset y_\nu \bar{L} \tilde{H} \nu_s + \frac{m_s}{2} \bar{\nu}_s^c \nu_s, \quad (1)$$

where  $H$  and  $L$  are the  $SU(2)_L$  Higgs and lepton doublets respectively,  $y_\nu$  is the neutrino Dirac Yukawa matrix, and  $m_s$  is the Majorana mass term.

At the low-scales relevant for our analysis, the main effect of Eq. (1) is encoded in the active-sterile mixing angle. The parameter space SNe are most sensitive to, in the case of sterile-active mixing with electron ( $\sin^2 \theta_e$ ) is already strongly constrained from the terrestrial probes. In absence of muons in the SNe, the cases for sterile-active mixing with muon or tau neutrino are equivalent. In the former case, presence of muons can lead to extra channels for sterile neutrino production through charged-current interactions. Therefore in this work, we assume that the sterile neutrino mixes exclusively only with  $\nu_\tau$ . In terms of mass eigenstates  $\nu_1$  and  $\nu_2$ ,

$$\begin{aligned}\nu_\tau &= \cos \theta_\tau \nu_1 + \sin \theta_\tau \nu_2 \\ \nu_s &= -\sin \theta_\tau \nu_1 + \cos \theta_\tau \nu_2\end{aligned}\quad (2)$$

where  $\sin \theta_\tau$  denotes the mixing angle between the sterile and the tau neutrino.

**Low-Energy Supernovae.** While SN1987A was unique in its promity, SNe are not rare and can be used to study sterile neutrinos. We focus on a sub-class of core-collapse SNe with low-explosion energies, sometimes called underluminous Type IIP SNe, where the Type II represents the presence of hydrogen in the spectra and the P represents the SN's light-curve displaying a flat, or *plateau*, shape in time. The luminosity and duration of the plateau reflects the explosion energy, ejecta mass, nickel  $^{56}\text{Ni}$  mass and progenitor radius. Therefore, the explosion energy can be inferred given the spectrum and the light curves. For example Refs. [29–32] used fitting formulae, simulations, and statistical inference along with quantifying the uncertainties, to infer the most likely explosion energies for a collection of Type IIP SNe. The inferred explosion energy  $E_{obs}$  ranges from  $7.4 \times 10^{49}$  erg to  $4 \times 10^{51}$  erg. While the upper end of the reconstructed energies are larger than typical predictions of numerical simulations, the lower end is approximately consistent with various simulated SNe. Here, we are interested in sterile neutrinos produced in the core which can decay and deposit energies of a similar magnitude, and hence can be constrained from the observa-

tions of low-energy SNe by requiring  $E_{dep} < 10^{50}$  erg. Since numerical simulations are typically under-powered compared to observations, we expect our constraints to be conservative, unless some surprising systematic over-evaluation is discovered in simulations.

We will examine two massive stars with initial masses  $8.8M_\odot$  and  $18.8M_\odot$  for obtaining bounds on the sterile neutrino parameter space. There are several reasons for these choices. First, the SN explosion energy is not a simple monotonic function of the initial mass of the progenitor. Instead, the explosion energy depends on the structure of the inner few solar masses of the progenitor's core, which in turn depends in a complex way to the progenitor mass, metallicity or even final hydrogen mass [29, 33]. Second, light progenitors have a systematically different core structure to those of Fe cored stars [34] which collapse by electron capture on its ONeMg core, which typically explode more readily [35, 36]. Our adopted  $8.8M_\odot$  progenitor aims to model this. Similarly, we adopt the  $18.8M_\odot$  as the typical massive star which evolves into a supergiant where its Fe core collapses causing a Type IIP SN. Finally, estimates of the progenitor masses of underluminous Type IIP supernovae cover a range: for example, SN1997D with estimated energy  $1.0 \times 10^{50}$  erg has an estimated initial mass  $10 \pm 2M_\odot$  [37], while SN2003Z has estimated  $1.6 \times 10^{50}$  erg and  $14.15 \pm 0.95M_\odot$  [38] and SN2008kb  $1.8 \times 10^{50}$  erg and  $12.15 \pm 0.75M_\odot$  [38]. We thus consider the reality of the progenitors of underluminous Type IIP to lie somewhere between our adopted  $8.8M_\odot$  and  $18.8M_\odot$  progenitors.

**Energy Deposition.** Since the explosion energies of SN IIP are inferred from the light curves and dependent on the ejecta mass and the amount of  $^{56}\text{Ni}$  synthesized in the outer envelope, the limit on the energy deposition by any exotic species is constrained to the mantle region of the SN; in other words, we consider species which escape beyond the photosphere will simply present an energy sink for the explosion. The total energy deposited by sterile neutrino produced in the SN core, decaying outside the core but inside the SN envelope region ( $R_{core} < r < R_{env}$ ) is given by

$$E_{dep} = \eta_{\text{lapse}}^2 \int dt \int_0^{R_{core}} dr \int_{m_s}^\infty dE_s \frac{dL_s(r, E_s, t)}{dr dE_s} \Theta \left( E_s - \frac{m_s}{\eta_{\text{lapse}}} \right) \times \left\{ \exp \left[ -\frac{(R_{core} - r)}{L_{decay}} \right] - \exp \left[ -\frac{(R_{env} - r)}{L_{decay}} \right] \right\}, \quad (3)$$

where  $\eta_{\text{lapse}}$  is the gravitational redshift factor,  $E_s$  is the sterile neutrino energy,  $\frac{dL_s(r, E_s, t)}{dr dE_s}$  is gradient of the differential sterile neutrino luminosity,  $\Theta(x)$  is the Heaviside theta function and  $L_{decay}$  is the decay length. Note that at large mixing angles, the decay length becomes comparable to the PNS radius and our treatment should not be taken as rigorous. We hope to return to this trapping

regime in future work with greater precision.

Sterile neutrinos produced in the SN core will also have to overcome the strong gravitational attraction arising from such high matter densities to avoid trapping. If sterile neutrino energy is sufficiently small,  $E_s < m_s/\eta_{\text{lapse}}$ , it will be gravitationally trapped inside the SN core. The *lapse* factor  $\eta_{\text{lapse}}$  is the conversion factor relating the energy measured locally in the SN frame to

the energy measured at the same point by an observer at infinity. For example in the weak-field limit of the Schwarzschild metric, the gravitational lapse factor is given by  $\eta_{\text{lapse}} \simeq m_s(1 + GM(r)/r)$ . We also need to correct for the difference between the local time and the observer time in the energy emission rate. Both of these effects taken together lead to the inclusion of  $\eta_{\text{lapse}}^2$  in the expression for  $E_{\text{dep}}$ . In our case, we find that our results are sensitive to the gravitational trapping (inside the core) only for very heavy steriles ( $> 300$  MeV). Therefore, the results in absence of the gravitational trapping factor will be almost similar.

**Sterile Neutrino Production.** In a SN core, sterile neutrinos can be produced by  $e^+e^-$  or neutrino pair annihilation and the inelastic scattering of (anti-)neutrinos. Since  $n, p, e^+, e^-, \nu_e, \bar{\nu}_e$  are degenerate in the hot proto-neutron star core, Pauli-blocking will render pair-annihilation and inelastic scattering on the non-degenerate neutrino species ( $\nu_\mu, \nu_\tau$ ) the dominant processes for  $\nu_s$  production [8, 9, 19, 39]. The amplitude for these relevant processes is given in Table. I, in terms of Mandelstam variables. Note that we have explicitly listed the charge-conjugated processes in order to avoid any confusion.

Process	$S M ^2/(8G_F^2 \sin^2 \theta_\tau)$
$\nu_\tau + \bar{\nu}_\tau \rightarrow \nu_s + \bar{\nu}_\tau$	$4u(u - m_s^2)$
$\nu_\tau + \bar{\nu}_\tau \rightarrow \nu_s + \nu_\tau$	$4u(u - m_s^2)$
$\nu_\mu + \bar{\nu}_\mu \rightarrow \nu_s + \bar{\nu}_\tau$	$u(u - m_s^2)$
$\nu_\mu + \bar{\nu}_\mu \rightarrow \nu_s + \nu_\tau$	$u(u - m_s^2)$
$\nu_\tau + \bar{\nu}_\tau \rightarrow \nu_s + \nu_\tau$	$2s(s - m_s^2)$
$\bar{\nu}_\tau + \bar{\nu}_\tau \rightarrow \nu_s + \bar{\nu}_\tau$	$2s(s - m_s^2)$
$\nu_\mu + \bar{\nu}_\tau \rightarrow \nu_s + \nu_\mu$	$s(s - m_s^2)$
$\bar{\nu}_\mu + \bar{\nu}_\tau \rightarrow \nu_s + \bar{\nu}_\mu$	$s(s - m_s^2)$
$\nu_\tau + \bar{\nu}_\mu \rightarrow \nu_s + \bar{\nu}_\mu$	$u(u - m_s^2)$
$\nu_\mu + \bar{\nu}_\tau \rightarrow \nu_s + \nu_\mu$	$u(u - m_s^2)$

Table I. Matrix element squared  $S|M|^2$  for the dominant processes involved in sterile neutrino production in terms of Mandelstam variables, in units of  $8G_F^2 \sin^2 \theta_\tau$ .

*Boltzmann Transport.* The evolution of sterile neutrino abundances is governed by the Boltzmann transport equation. Since solving the exact transport equation for sterile neutrino is not possible, we simplify the task at hand by assuming the medium is homogeneous and isotropic [40]. This implies that the change in phase-space density will only be affected by the scatterings/pair-annihilation processes in the SN core. In this case, the simplified kinetic equation for sterile neutrino production is

$$\frac{\partial f_s}{\partial t} = \mathcal{C}_{\text{coll}}(f_s), \quad (4)$$

where  $f_s$  is the sterile neutrino phase-space density distribution and  $\mathcal{C}_{\text{coll}}$  is the sum of all possible collisional

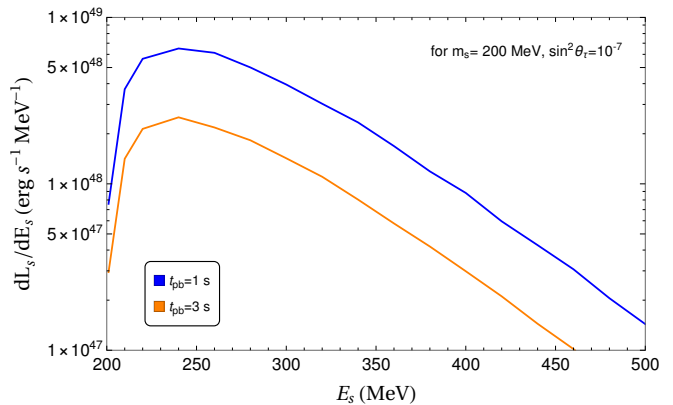


Figure 2. Differential sterile neutrino luminosity for sterile neutrino mass  $m_s = 200$  MeV and  $\sin^2 \theta_\tau = 10^{-7}$  at different post-bounce times, see e.g., Eq. (6).

interactions. In our case, the collisional term for  $2 \rightarrow 2$  particle interactions can be written as

$$\mathcal{C}_{\text{coll}} = \frac{1}{2E_s} \int d^3 \tilde{p}_2 d^3 \tilde{p}_3 d^3 \tilde{p}_4 \Lambda(f_s, f_2, f_3, f_4) \times S|M|_{12 \rightarrow 34}^2 \delta^4(p_s + p_2 - p_3 - p_4) (2\pi^4), \quad (5)$$

where  $d^3 \tilde{p}_i = d^3 p_i / ((2\pi^3) 2E_i)$ ,  $\Lambda(f_s, f_2, f_3, f_4) = (1 - f_s)(1 - f_2)f_3f_4 - f_s f_2(1 - f_3)(1 - f_4)$  is the phase-space factor including the Pauli blocking of the final states,  $S$  is the symmetry factor,  $|M|^2$  is the interaction matrix element squared,  $E_i$  and  $p_i$  are energy and momentum of the  $i$ -th particle with subscript label  $s$  for sterile neutrino. For the range of interest for  $\sin^2 \theta_\tau$ , the sterile neutrino produced will not be trapped in the SN, hence we can safely assume  $f_s = 0$ . After numerically solving for  $f_s$ , we can calculate the sterile neutrino luminosity  $\frac{dL_s}{dE_s}$  as [19, 41]

$$\frac{dL_s}{dE_s} = \frac{2E_s}{\pi} \int dr r^2 \frac{df_s}{dt} E_s p_s. \quad (6)$$

As an example, we show this differential and integrated sterile neutrino luminosity in Figs. 2 and 3, respectively for reference sterile neutrino mass  $m_s = 200$  MeV.

*Visible Energy Deposition.* The sterile neutrino decays and deposits energy into the SN envelope. For the mass range of interest and mixing only with  $\nu_\tau$ , the charged-current processes are kinematically forbidden. Therefore, we only consider following neutral current decays and their charge-conjugate processes, assuming  $\nu_s$  to be Majorana particles [42–46]. Note that the analytical expressions for  $\pi^0$  decay mode width in Refs. [42, 44, 45] differ by a factor of 2 (in the numerator) compared to Refs [43, 46]. In this work, we use expressions given in

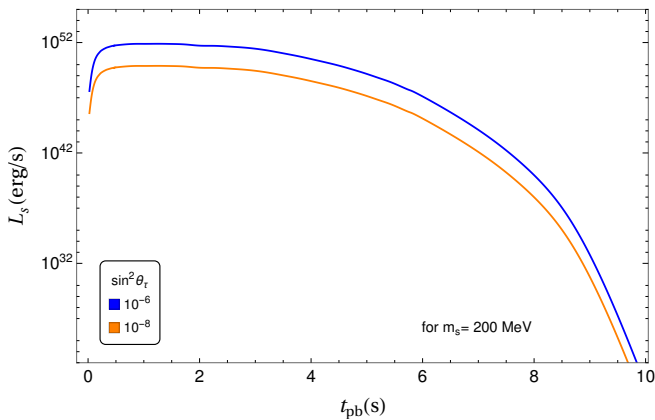


Figure 3. Integrated sterile neutrino luminosity plotted as a function of post-bounce time for sterile neutrino mass  $m_s = 200$  MeV for different  $\sin^2 \theta_\tau$ , see Eq. (6).

Ref. [45]. The relevant decay modes for  $\nu_s$  are

$$\begin{aligned}
 \nu_s &\rightarrow \nu_\tau \pi^0, \\
 \nu_s &\rightarrow \nu_\tau e^+ e^-, \\
 \nu_s &\rightarrow \nu_\tau \mu^+ \mu^-, \\
 \nu_s &\rightarrow \nu_\tau \nu_x \bar{\nu}_x,
 \end{aligned}
 \tag{7}$$

where  $x = (e, \mu, \tau)$ . The process involving neutral pion tends to be the dominant decay mode for higher masses while the electron channel contributes negligibly to the decay width. We classify the first 3 listed processes as the *visible* decay modes while the last decay mode entirely into neutrinos as *invisible*. Based on this classification, we will discuss two limiting cases of energy deposition, *i*) the entire energy from sterile decay is deposited, and *ii*) only the *visible* decay modes deposit their energy into the SN envelope. The energy deposition in the latter case is determined by the branching ratio into the *visible* modes, given by

$$BR_{vis} = 1 - \frac{\Gamma(\nu_s \rightarrow \nu_\tau \nu_x \bar{\nu}_x)}{\Gamma_{tot}},
 \tag{8}$$

where  $\Gamma_{tot}$  is the total decay width calculated from all four decay modes.

We now discuss the efficacy of the branching ratio method. Two possible issues can be raised for this approach. Firstly, the presence of a neutrino final state in the the first 3 decay modes might take away a portion of the (assumed to-be) deposited energy. Secondly, there might be possible energy deposition into the mantle from the secondary neutrinos produced in the invisible decay channel. Before we address both of these issues, a crucial fact to remember is that neutrinos can get trapped or multiply scatter in the hot and highly dense SN environment, conditions for which can mainly occur in/near the proto-neutron star core. In the first case for  $m_s \geq m_\pi$ , the decays of the sterile neutrino are dominated by the pion mode. For mixing angles of interest, such steriles

decay far inside the  $R_{env}$ , which gives  $\nu_\tau$  produced to encounter high densities and undergo to at least one scattering to deposit substantial energy into the envelope<sup>1</sup>. For  $m_s \leq m_\pi$ , the decays are dominated by the  $3\nu$  mode, with average neutrino energy  $\sim 80$  MeV. Such energetic neutrinos would have been trapped if produced near the core but for lighter  $\nu_s$  (and relevant mixings), the average decay length is far outside the SN. Hence, a major portion of the neutrino energy will not be deposited and hence considering this channel as “invisible” is a good approximation. From the above discussion, we can conclude that the branching ratio method is a good estimator of the actual energy deposition from sterile neutrino decays. A proper inclusion of secondary neutrino energy deposition is beyond the scope of the current work and we stress that it should not affect very strongly the results presented here.

**Reference SN Model** In this work, we adopt two different SN profiles to obtain the bounds in the mixing-mass plane as well as to test the robustness of the bounds to the SN profile used. Since we are concerned with very small mixing angles, we assume that the  $\nu_s$  production does not affect the standard SN processes. In the *Garching model*, we apply our reasoning to obtain realistic bounds with the SFHo-18.8 model simulated by the Garching group, which adopts a  $18.8 M_\odot$  progenitor and includes six-species neutrino transport [47–49]. The SFHo EoS [50] is used and PNS convection is modeled by a mixing-length treatment [51]. We use the simulated SN evolution assuming  $R_{core} \sim 20$  km for all post-bounce time sequences up to  $\sim 10$ s and envelope extending up to  $\sim 5 \times 10^7$  km.

We also consider a  $8.8 M_\odot$  SN profile [52] (which is on the lower end of the progenitor mass range that finally end up in a neutron star) to study the effect of progenitor dependence on our bounds. This profile collapses via electron-capture on its ONeMg core with a final baryonic mass of  $1.366 M_\odot$  using Shen’s stiff baryonic equation of state [53] for hot dense nuclear matter and a final neutron star radius of about 15 km. Also note that unlike the  $18.8 M_\odot$  progenitor model, this simulated profile does not include muons or convection in proto-neutron star. Although both of these models have peak temperatures of about 30 – 40 MeV, we find quite different bounds in each case (See Fig. 1 and discussion on results).

The sterile neutrino production rate depends mainly on the sterile energy, sterile mass and the radial distribution of temperature. For SFHo-18.8, the outer layer of the core is the hottest in the first few time steps, as the in-falling matter towards the iron core first heats up the core

<sup>1</sup> Note that our discussion only centers around the decay lengths for the average secondary neutrino energies in a distribution. Some of these neutrinos if not being trapped/scatter, doesn’t imply all of the produced neutrino in the decay mode under consideration will free stream. The higher end tail of the energy spectrum will most likely be deposited.

edge. Thus, the maximum production occurs at edges of the core for the first few ms after  $t_{pb} = 0$ . But as the inner core gets hotter with time, the maximum production rate shifts closer to the center. The total production rate grows with time up to  $\sim 3 - 4$  s after which it falls off rapidly.

It is easy to see that for masses  $m_s \lesssim T$ , the high energy sterile states can be produced easily. For heavier steriles, although mainly produced at rest, energies up to  $\sim (6 - 8)T$  are feasible (since production is through  $2 \rightarrow 2$  scattering processes). However, some higher energy states for heavier steriles can still be produced with modest Boltzmann suppression.

**Results.** We display our main results in Fig. 1 while only assuming non-zero tau neutrino mixing. For the blue curves (both  $8.8$  and  $18.8 M_\odot$  progenitor), we assume no more than  $10^{50}$  erg energy deposition, and only include contributions from the electromagnetic decay products of the sterile. For  $18.8 M_\odot$  progenitor, we see that this constraint can be close to two orders of magnitude stronger than the energy loss bounds obtained from SN1987A [19], and provides the leading constraint on the mixing angle for  $15 \text{ MeV} \lesssim m_s \lesssim 400 \text{ MeV}$ . This constraint could be yet stronger if all the sterile decay products including the active neutrinos deposit energy in the envelope (black dashed curve). Finally, for the other blue curve we see that the bound is significantly weakened if the progenitor mass is lowered to  $8.8 M_\odot$ . It should be noted however that even in this case, our results provide the leading constraint in the 100-400 MeV mass window. Also included in Fig. 1 is the region favored by Type-I seesaw models for neutrino masses (dashed brown curves), BBN bounds assuming standard cosmology [21–23], T2K [24] and BEBC bounds [25]. We note that BBN bounds exclude the region below the green curve in Fig. 1. However, in the presence of a lepton asymmetry these constraints can be substantially weakened [54].

We again note that bounds depend on the progenitor model. This is due to the fact that sterile neutrino production depends sensitively on  $T$ . The temperature profiles for  $18.8 M_\odot$  SN have consistently higher temperatures for all  $t = (0 - 10)$ s as compared to the  $8.8 M_\odot$  progenitor.

We note that while we have fixed to mass-mixing with the tau-neutrino in Fig. 1, we expect qualitatively similar results for mixing with the muon-neutrino.

**Future directions.** The present paper has examined the implications of heavy sterile neutrinos for low-energy SNe. This work can be extended in a number of directions. For one, we have only mixing with one active neutrino flavor at a time. It would be worthwhile to examine more generic flavor structure assumptions. Secondly, it is possible that the production and decay of sterile neutrinos is not controlled by the EW force. For example, sterile transition magnetic moments have been widely studied [55–58]. We also anticipate low-energy SNe placing stringent constraints on transition magnetic moments.

Moreover, even while restricting to mass-mixing, there are additional avenues to be explored. Given that SNe are efficient production sites of sterile neutrinos, the impact of the escaping sterile neutrinos (and their decay products) could be significant. In particular, for axions it is known that requiring that the axions not produce a photon flux above the diffuse gamma-ray background leads to strong bounds at low masses [59]. Secondly, the high-energy neutrino flux produced by the decaying sterile neutrinos may also be detectable at future neutrino experiments like DUNE and Hyper-K [19], and a detailed follow-up in light of our results may yield new constraints.

**Conclusions.** We have found that low-energy SNe can provide leading constraints on sterile neutrinos in the 15-400 MeV range. In addition, these bounds probe theoretically well-motivated parameter space predicted by Type-I seesaw models of neutrino masses. In future work we plan to return to this scenario and explore implications of the neutrino and gamma-rays emerging from sterile decays beyond the SN envelope.

**Acknowledgements.** We are very grateful to Anna Suliga for helpful discussions and comments. We thank Hans-Thomas Janka and Daniel Kresse for providing the SN profiles used in this work. The work of GC is supported by the U.S. Department of Energy under the award number DE-SC0020250 and DE-SC0020262. The works of SH, PH, and IMS are supported by the U.S. Department of Energy Office of Science under award number DE-SC0020262 and DE-SC0020250. The work of SH is also supported by NSF Grant No. AST1908960, No. PHY-1914409 and No. PHY-2209420; and JSPS KAKENHI Grant Numbers JP22K03630 and JP23H04899. This work was supported by World Premier International Research Center Initiative (WPI Initiative), MEXT, Japan.

- 
- [1] S. Dodelson and L. M. Widrow, *Sterile-neutrinos as dark matter*, *Phys. Rev. Lett.* **72** (1994) 17 [hep-ph/9303287].
  - [2] X.-D. Shi and G. M. Fuller, *A New dark matter candidate: Nonthermal sterile neutrinos*, *Phys. Rev. Lett.* **82** (1999) 2832 [astro-ph/9810076].
  - [3] E. K. Akhmedov, V. A. Rubakov and A. Y. Smirnov, *Baryogenesis via neutrino oscillations*, *Phys. Rev. Lett.* **81** (1998) 1359 [hep-ph/9803255].
  - [4] P. D. Bolton, F. F. Deppisch and P. S. Bhupal Dev, *Neutrinoless double beta decay versus other probes of heavy sterile neutrinos*, *JHEP* **03** (2020) 170 [1912.03058].
  - [5] A. M. Abdullahi et al., *The present and future status of heavy neutral leptons*, *J. Phys. G* **50** (2023) 020501 [2203.08039].
  - [6] M. A. Acero et al., *White Paper on Light Sterile Neutrino Searches and Related Phenomenology*,

- 2203.07323.
- [7] G. Chauhan and T. Steingasser, *Gravity-improved metastability bounds for the Type-I Seesaw Mechanism*, *2304.08542*.
- [8] G. M. Fuller, A. Kusenko and K. Petraki, *Heavy sterile neutrinos and supernova explosions*, *Phys. Lett. B* **670** (2009) 281 [0806.4273].
- [9] T. Rembiaz, M. Obergaulinger, M. Masip, M. A. Pérez-García, M.-A. Aloy and C. Albertus, *Heavy sterile neutrinos in stellar core-collapse*, *Phys. Rev. D* **98** (2018) 103010 [1806.03300].
- [10] J. Hidaka and G. M. Fuller, *Sterile Neutrino-Enhanced Supernova Explosions*, *Phys. Rev. D* **76** (2007) 083516 [0706.3886].
- [11] I. Tamborra, G. G. Raffelt, L. Hudepohl and H.-T. Janka, *Impact of eV-mass sterile neutrinos on neutrino-driven supernova outflows*, *JCAP* **01** (2012) 013 [1110.2104].
- [12] G. G. Raffelt and S. Zhou, *Supernova bound on keV-mass sterile neutrinos reexamined*, *Phys. Rev. D* **83** (2011) 093014 [1102.5124].
- [13] A. M. Suliga, I. Tamborra and M.-R. Wu, *Lifting the core-collapse supernova bounds on keV-mass sterile neutrinos*, *JCAP* **08** (2020) 018 [2004.11389].
- [14] C. A. Argüelles, V. Brdar and J. Kopp, *Production of keV Sterile Neutrinos in Supernovae: New Constraints and Gamma Ray Observables*, *Phys. Rev. D* **99** (2019) 043012 [1605.00654].
- [15] A. M. Suliga, I. Tamborra and M.-R. Wu, *Tau lepton asymmetry by sterile neutrino emission – Moving beyond one-zone supernova models*, *JCAP* **12** (2019) 019 [1908.11382].
- [16] V. Syvolap, O. Ruchayskiy and A. Boyarsky, *Resonance production of keV sterile neutrinos in core-collapse supernovae and lepton number diffusion*, *Phys. Rev. D* **106** (2022) 015017 [1909.06320].
- [17] S. W. Falk and D. N. Schramm, *Limits From Supernovae on Neutrino Radiative Lifetimes*, *Phys. Lett. B* **79** (1978) 511.
- [18] A. D. Dolgov, S. H. Hansen, G. Raffelt and D. V. Semikoz, *Heavy sterile neutrinos: Bounds from big bang nucleosynthesis and SN1987A*, *Nucl. Phys. B* **590** (2000) 562 [hep-ph/0008138].
- [19] L. Mastrototaro, A. Mirizzi, P. D. Serpico and A. Esmaili, *Heavy sterile neutrino emission in core-collapse supernovae: Constraints and signatures*, *JCAP* **01** (2020) 010 [1910.10249].
- [20] A. Caputo, H.-T. Janka, G. Raffelt and E. Vitagliano, *Low-Energy Supernovae Severely Constrain Radiative Particle Decays*, *Phys. Rev. Lett.* **128** (2022) 221103 [2201.09890].
- [21] A. Boyarsky, O. Ruchayskiy and M. Shaposhnikov, *The Role of sterile neutrinos in cosmology and astrophysics*, *Ann. Rev. Nucl. Part. Sci.* **59** (2009) 191 [0901.0011].
- [22] O. Ruchayskiy and A. Ivashko, *Restrictions on the lifetime of sterile neutrinos from primordial nucleosynthesis*, *JCAP* **10** (2012) 014 [1202.2841].
- [23] N. Sabti, A. Magalich and A. Filimonova, *An Extended Analysis of Heavy Neutral Leptons during Big Bang Nucleosynthesis*, *JCAP* **11** (2020) 056 [2006.07387].
- [24] T2K collaboration, *Search for heavy neutrinos with the T2K near detector ND280*, *Phys. Rev. D* **100** (2019) 052006 [1902.07598].
- [25] R. Barouki, G. Marocco and S. Sarkar, *Blast from the past II: Constraints on heavy neutral leptons from the BEBC WA66 beam dump experiment*, *SciPost Phys.* **13** (2022) 118 [2208.00416].
- [26] P. Minkowski,  *$\mu \rightarrow e\gamma$  at a Rate of One Out of  $10^9$  Muon Decays?*, *Phys. Lett. B* **67** (1977) 421.
- [27] M. Gell-Mann, P. Ramond and R. Slansky, *Complex Spinors and Unified Theories*, *Conf. Proc. C* **790927** (1979) 315 [1306.4669].
- [28] R. N. Mohapatra and G. Senjanovic, *Neutrino Mass and Spontaneous Parity Nonconservation*, *Phys. Rev. Lett.* **44** (1980) 912.
- [29] O. Pejcha and J. L. Prieto, *On The Intrinsic Diversity of Type II-Plateau Supernovae*, *Astrophys. J.* **806** (2015) 225 [1501.06573].
- [30] T. Müller, J. L. Prieto, O. Pejcha and A. Clocchiatti, *The Nickel Mass Distribution of Normal Type II Supernovae*, *Astrophys. J.* **841** (2017) 127 [1702.00416].
- [31] J. A. Goldberg, L. Bildsten and B. Paxton, *Inferring Explosion Properties from Type II-Plateau Supernova Light Curves*, *Astrophys. J.* **879** (2019) 3 [1903.09114].
- [32] J. W. Murphy, Q. Mabanta and J. C. Dolence, *A Comparison of Explosion Energies for Simulated and Observed Core-Collapse Supernovae*, *Mon. Not. Roy. Astron. Soc.* **489** (2019) 641 [1904.09444].
- [33] T. Sukhbold and S. Woosley, *The Compactness of Presupernova Stellar Cores*, *Astrophys. J.* **783** (2014) 10 [1311.6546].
- [34] S. Jones et al., *Advanced Burning Stages and Fate of 8-10  $M_{\odot}$  Stars*, *Astrophys. J.* **772** (2013) 150 [1306.2030].
- [35] F. S. Kitaura, H.-T. Janka and W. Hillebrandt, *Explosions of O-Ne-Mg cores, the Crab supernova, and subluminescent type II-P supernovae*, *Astron. Astrophys.* **450** (2006) 345 [astro-ph/0512065].
- [36] L. Hudepohl, B. Müller, H. T. Janka, A. Marek and G. G. Raffelt, *Neutrino Signal of Electron-Capture Supernovae from Core Collapse to Cooling*, *Phys. Rev. Lett.* **104** (2010) 251101 [0912.0260].
- [37] N. N. Chugai and V. P. Utrobin, *The nature of sn 1997d: low mass progenitor and weak explosion*, *Astron. Astrophys.* **354** (2000) 557 [astro-ph/9906190].
- [38] M. L. Pumo, L. Zampieri, S. Spiro, A. Pastorello, S. Benetti, E. Cappellaro et al., *Radiation-hydrodynamical modelling of underluminous type II plateau Supernovae*, *Mon. Not. Roy. Astron. Soc.* **464** (2017) 3013 [1610.02981].
- [39] V. Syvolap, *Testing heavy neutral leptons produced in the supernovae explosions with future neutrino detectors*, *2301.07052*.
- [40] S. Hannestad and J. Madsen, *Neutrino decoupling in the early universe*, *Phys. Rev. D* **52** (1995) 1764 [astro-ph/9506015].
- [41] I. Tamborra, L. Hudepohl, G. Raffelt and H.-T. Janka, *Flavor-dependent neutrino angular distribution in core-collapse supernovae*, *Astrophys. J.* **839** (2017) 132 [1702.00060].
- [42] D. Gorbunov and M. Shaposhnikov, *How to find neutral leptons of the  $\nu$ MSM?*, *JHEP* **10** (2007) 015 [0705.1729].
- [43] A. Atre, T. Han, S. Pascoli and B. Zhang, *The Search for Heavy Majorana Neutrinos*, *JHEP* **05** (2009) 030 [0901.3589].
- [44] K. Bondarenko, A. Boyarsky, D. Gorbunov and O. Ruchayskiy, *Phenomenology of GeV-scale Heavy*



- Neutral Leptons*, *JHEP* **11** (2018) 032 [1805.08567].
- [45] P. Coloma, E. Fernández-Martínez, M. González-López, J. Hernández-García and Z. Pavlovic, *GeV-scale neutrinos: interactions with mesons and DUNE sensitivity*, *Eur. Phys. J. C* **81** (2021) 78 [2007.03701].
- [46] J. C. Helo, S. Kovalenko and I. Schmidt, *Sterile neutrinos in lepton number and lepton flavor violating decays*, *Nucl. Phys. B* **853** (2011) 80 [1005.1607].
- [47] “Garching core-collapse supernova research archive.” <https://wwwmpa.mpa-garching.mpg.de/ccsnarchive/>.
- [48] A. Mirizzi, I. Tamborra, H.-T. Janka, N. Saviano, K. Scholberg, R. Bollig et al., *Supernova Neutrinos: Production, Oscillations and Detection*, *Riv. Nuovo Cim.* **39** (2016) 1 [1508.00785].
- [49] R. Bollig, W. DeRocco, P. W. Graham and H.-T. Janka, *Muons in Supernovae: Implications for the Axion-Muon Coupling*, *Phys. Rev. Lett.* **125** (2020) 051104 [2005.07141].
- [50] A. W. Steiner, M. Hempel and T. Fischer, *Core-collapse supernova equations of state based on neutron star observations*, *Astrophys. J.* **774** (2013) 17 [1207.2184].
- [51] R. Bollig, H. T. Janka, A. Lohs, G. Martínez-Pinedo, C. J. Horowitz and T. Melson, *Muon Creation in Supernova Matter Facilitates Neutrino-driven Explosions*, *Phys. Rev. Lett.* **119** (2017) 242702 [1706.04630].
- [52] L. Hüdepohl, B. Müller, H. T. Janka, A. Marek and G. G. Raffelt, *Neutrino Signal of Electron-Capture Supernovae from Core Collapse to Cooling*, *Phys. Rev. Lett.* **104** (2010) 251101 [0912.0260].
- [53] H. Shen, H. Toki, K. Oyamatsu and K. Sumiyoshi, *Relativistic equation of state of nuclear matter for supernova and neutron star*, *Nucl. Phys. A* **637** (1998) 435 [nucl-th/9805035].
- [54] G. B. Gelmini, M. Kawasaki, A. Kusenko, K. Murai and V. Takhistov, *Big Bang Nucleosynthesis constraints on sterile neutrino and lepton asymmetry of the Universe*, *JCAP* **09** (2020) 051 [2005.06721].
- [55] S. N. Gninenko and N. V. Krasnikov, *Limits on the magnetic moment of sterile neutrino and two photon neutrino decay*, *Phys. Lett. B* **450** (1999) 165 [hep-ph/9808370].
- [56] P. Coloma, P. A. N. Machado, I. Martínez-Soler and I. M. Shoemaker, *Double-Cascade Events from New Physics in Icecube*, *Phys. Rev. Lett.* **119** (2017) 201804 [1707.08573].
- [57] G. Magill, R. Plestid, M. Pospelov and Y.-D. Tsai, *Dipole Portal to Heavy Neutral Leptons*, *Phys. Rev. D* **98** (2018) 115015 [1803.03262].
- [58] V. Brdar, A. de Gouvêa, Y.-Y. Li and P. A. N. Machado, *Neutrino magnetic moment portal and supernovae: New constraints and multimessenger opportunities*, *Phys. Rev. D* **107** (2023) 073005 [2302.10965].
- [59] A. Caputo, G. Raffelt and E. Vitagliano, *Muonic boson limits: Supernova redux*, *Phys. Rev. D* **105** (2022) 035022 [2109.03244].